Preparation of new copolymer (polystyrene/TMSPM grafted on DDA-fractionated algerian montmorillonite) hybrid organoclay by radical copolymerization: structural study, thermal stability and hydrophobicity area

Azzedine Melouki[1] · Smail Terchi[2] · Dehimi Ouali[1] · Abdelhakim Bounab[3]

Abstract

Polystyrene/organo-Algerian montmorillonite hybrid material was prepared by radical copolymerization of styrene monomer in the presence of the double organic modified clay. Before copolymerization process, the local (Algerian) montmorillonite was sodified, fractionated (< 2 μm), intercaled with dodecylamine (DDA) salts and grafted by trimethoxysilylpropylmethacrylate (TMSPM). The copolymerization has occurred onto methacrylate ported by grafted silane. X-ray fluorescence results showed a successful homoionization and insersion of DDA salts onto montmorillonite. CHN microanalysis revealed the evolution of the carbon ratio during modification of MMT by DDA, grafting and copolymerization reactions. The characterization (XRD) revealed that DDA salts were intercaled onto montmorillonite galleries and part of the copolymerization was occurred in interlayer spaces of clay (intercalated structure) by increasing d_{001} from 12.69 Å for homoionised clay to 15.33 Å for intercalated clay and to 23.08 Å for hybrid material. Fourier transform infrared (FTIR) spectra mainly confirmed the presence of DDA salts, the grafting of TMSPM and polystyrene polymer and increasing of hydrophobicity of clay during modifications process (intercalation, grafting and copolymerization). Thermogravimetic analysis (TGA) showed that the grafted clay sample have higher thermal stability than intercalated sodic montmorillonite. TGA revealed also that the thermal stability of prepared hybrid organoclay is greatly higher than pur polystyrene polymer (45 °C higher) and that hydrophobicity$_{hybrid\ organoclay}$ > hydrophobicity$_{grafted\ clay}$ > hydrophobicity $_{intercalated\ clay}$ > hydrophobicity$_{fractinated\ sodic\ clay}$. The copolymer was recovered by hydrofluoric acid attack, analyzed by FTIR and compared to hybrid organoclay FTIR spectra.

Keywords Thermal stability · Hybrid materials · TG analysis · Grafting · Radical copolymerization

Introduction

Organoclay materials were obtained by modifying the surface of clay minerals with organic compounds. They have different applications in sciences and industries [1]. For example, they are used for water treatment [2–4] and polymers additives to prepare polymers/organoclays hybrid materials [5]. Among these clays, montmorillonite is one of the most common-type clays that is used to prepare the organoclays and organoclays/polymers hybrid materials [6–8]. The montmorillonite clay is a characteristic representative of aluminosilicates. It has several special properties: lamellar structure, swelling ability, special capacity of hydration, adsorption and a possibility of interlayer ion exchange. This latter property makes montmorillonite suitable and ready for possible modifications by cationics organics compounds such as alkylammoniums cations. This kind of mineral has an excess negative charge on its surface, where cations can be easily adsorbed [9].This surface charge can therefore be modified by carrying out the modification process with organic surfactants [10, 11]. A previous study has shown that modifications by quaternary alkylammonium

✉ Smail Terchi
smail.terchi@univ-msila.dz

1 Laboratoire de Matériaux Inorganique, Département de Chimie, Faculté de science, Université de M'Sila, M'Sila, Algérie

2 Département de Chimie, faculté de science, Université de M'Sila, M'Sila, Algérie

3 Département de Pharmacie, Université d'Alger, Algiers, Algérie

ions onto clay have been developed to improve the compatibility of clay minerals with less polar matrices [12]. In addition, this type of clay is universally abundant in nature and can be obtained in pure form at low cost. The montmorillonite is hydrophilic in nature and can only interact with hydrophilic polymers such as poly (ethylene oxide) or poly (vinyl alcohol). So it would be very difficult to mix these kinds of minerals with hydrophobic polymers. To overcome this obstacle and make possible organo-mineral interactions, hydrophobic groups should be introduced on the surfaces of the layers [13]. Previous studies have shown that the insertion of organic complexes between the layers of a montmorillonite changed the hydrophilic property of its surface making it hydrophobic [14].

This modification method may be possible by reacting silanes onto silanol groups (Si–OH) located on the sheets edges of this type of clay [15, 16] and on structural defects located on the external surfaces of the layers [17].

In previous study, the modification of montmorillonite by aminosilane reveals that the silane was intercaled in the interlayer spacing of montmorillonite due to the increase in the basal spacing, the high value of the latter can only be explained by the presence of a double layer of molecules of this silane connecting the two layers of clay [18].The technique consists of putting these silanols in contact with organosilane agents [19]. In the same context, studies have shown that the grafting of a silane such as aminopropyltrimethoxysilane onto montmorillonite caused the interlayer space to be inserted, increasing its d_{001}, [20], this confirms the possibility of having a grafting in the galleries of montmorillonite following a reaction between the silanol groups of the edges of the sheets and the alkoxy functions carried by the silicon of the silane, giving rise to bonds with covalent characters (Si–O–Si). It has also been shown that the montmorillonites having undergone surface modifications by silanes are thermally stable compared to montmorillonites having undergone conventional ion exchanges [21]. Most importantly, the characteristics of the modified clays can be easily adjusted through the introduction of various terminal groups of silane modifiers [13, 22]. Studies have shown that silane when added in high concentrations acts simultaneously on the silanols at the edges of the sheets and on the interlayer Si–O– [23]. These silanes, also called coupling agents, are polyvalent compounds. They represent an easy way to bond chemically polymers to silicas [24]. They can exist in the form of bifunctional monomers: an alkoxy upstream which can react with the silicic surface of clay and a function (vinyl, amine or thiol) downstream suitable for (co) polymerization with another vinyl monomer resulting in the synthesis of a organoclay hybrid material.

The scope of this study is to prepare a new organoclay hybrid material with high thermal stability and surface hydrophobicity, intended to be applied as catalytic supports in conversion reactions of organic compounds (acid–base properties) or added as additives in resins for surface protection for submerged objects such as submersible submarines.

In this study, we attempt to prepare a new hybrid organoclay material using a local (Algerian) montmorillonite,

for the first time. The organo-montmorillonite was prepared successively by the intercalation of dodecylamine (DDA) salts and grafting of trimethoxysilylpropylmethacrylate (TMSPM) on fractionated sodic montmorillonite.

The obtained organoclay which ported methacrylate group was dispersed in styrene monomer to prepare polystyrene/organoclay hybrid material via radical copolymerization. X-ray fluorescence (XRF) is used for characterization of raw clay, fractionated sodic clay and clay modified by DDA. CHN microanalysis is used for characterization of clay modified by DDA, grafted clay and hybrid material. X-ray diffraction XRD, Fourier transform infrared FTIR and thermogravimetic analysis TGA were used for characterization of all sample (raw, fractionated sodic, intercaled and grafted clay and hybrid material).

Experimental

Materials

The raw clay was purchased from the Maghnia deposit (West of Algeria).

The trimethoxysilylpropylmethacrylate TMSPM (98%, $d = 1.045$ g mL^{-1}), styrene monomer and dodecylamine DDA were purchased from Aldrich product.

The experimental protocol focused on preparation of different samples, namely raw clay (from the Maghnia deposit (West of Algeria)), purification and exchange of raw clay by sodium cations, intercalation of DDA onto Na-montmorillonite, grafting of TMSPM onto intercalated sample, the radical copolymerization to synthesis hybrid material sample and the dissolution of the latter by hydrofluoric acid in order to recover the organic part.

Purification of raw clay

The raw clay was washed with hydrogen peroxide to remove all organic matter followed by drying in an oven set at 80 °C for 24 h. The purified clay was milled in a mortar, in order to obtain homogeneous particle sizes. The obtained sample was denoted as raw Mt and characterized by elemental analysis (XRF), TGA, XRD and FTIR.

Sodification and fractionation of montmorillonite

The raw Mt sample was immersed into Nacl (1 M) solution. The contact was repeated three to four times for a better ion

exchange. The mixture was stirred for 20 min. It was filtered on a sintered glass and washed with distilled water using the centrifugation method (4000 rpm, for 20 min) until no chloride ion was detected with silver nitrate ($AgNO_3$) solution. The absence of the white precipitate is the confirmation of this. The mineral part was dried in oven at 80 °C for 24 h, milled with mortar and sieved (< 2 μm). The recovered powder is sodic montmorillonite (Mt-Na), which is characterized by chemical analysis, XRD, FTIR and TGA.

Mt-Na modified by DDA salts

30 g of Mt-Na was dispersed in 500 mL of hot water (80 °C) and stirred for 1 h (mixture A).

10 g of DDA was dissolved in a mixture of distilled water and hydrochloric acid (36%) at 80 °C for 3 h with stirring (mixture B). The obtained mixture (mixture A + B) was left at room temperature without stirring for about 24 h. The product was washed with distilled water at 80 °C until a negative chlorine test with $AgNO_3$. The precipitate was then centrifuged (4000 rpm, 20 min) and dried in an oven (80 °C, 24 h) to obtain the modified montmorillonite (Mt-DDA), which was characterized by microanalysis (CHN), XRD, FTIR and TGA.

Grafting of TMSPM onto Mt-DDA

10 g of the Mt-DDA was introduced into a two-pipe flask, immersed in an oil bath, equipped with a nitrogen inlet and a cooler equipped with a bubbler. 50 mL of freshly distilled Toluene (T_{eb}=110 °C) and 10 mg of hydroquinone (polymerization inhibitor) were added via a syringe via capillary.

The suspension was stirred for 15 min. Then, 8 mL (≈ 8 g) of TMSPM was added. The suspension was brought to reflux for 12 h under nitrogen sweeping at the temperature of 100 °C. Once this period was complete, the sample was cooled, filtered in a large sinter and then washed with dichloroethane (three times, 15 min) to eliminate the ungrafted monomer. The recovered sample was dried with a water pump for 6 h before putting in the oven (80 °C, 24 h) (Scheme 1a). This sample is denoted as Mt-TMSPM, which is characterized by microanalysis tests (C assay), XRD, FTIR and TGA.

Copolymerization of styrene onto Mt-TMSPM

5g of Mt-TMSPM, dried under vacuum, was introduced in a 50-mL flask with two tubes.

A determined amount of toluene (freshly distilled solvent) and 14 mL (12.7 g; d=0.906) of styrene monomer were introduced using a syringe and a capillary. The suspension was stirred, degassed by bubbling nitrogen for 30 min and heated at the polymerization temperature (65 °C). The appropriate amount of azo initiator such as azobisisobutyronitrile (AIBN) was dissolved in 3 mL of toluene was then added, with the ratio [styrene]/[AIBN] = 100.

The polymerization reaction was maintained for 24 h under inert atmosphere.

The suspension was then filtered, and the support was placed in a soxhlet for extraction of the ungrafted polymer.

The solvent used for the extraction is toluene, which solubilizes the ungrafted polymer and removes it from the surface of the support. Only the grafted polymer remains attached to the surface (Scheme 1b). The recovered sample
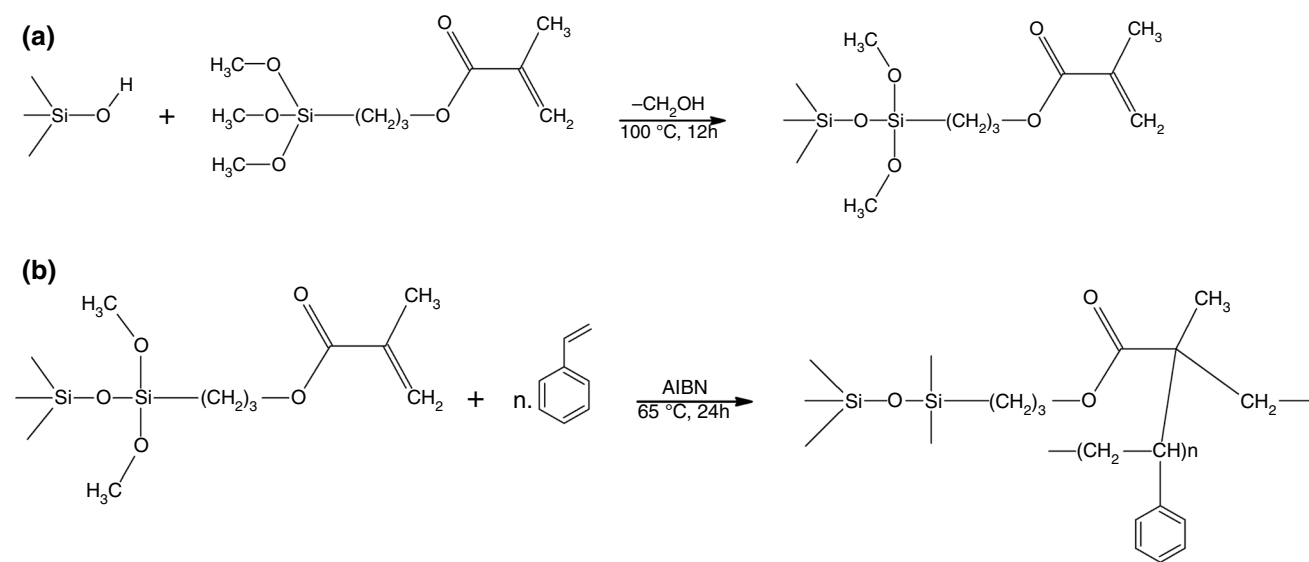
Scheme 1 Schematic illustration of grafting (**a**) and copolymerization (**b**) equations

is Hyb.Mat, oven-dried (80 °C, 24 h) and characterized by microanalysis, XRD, TGA and FTIR.

The blank PS with the same conditions without adding organo-MMT is prepared.

Dissolution of Hyb.Mat by hydrofluoric acid

1 g of Hyb.Mat was placed in a Teflon container fitted with an airtight cap. 10 mL of a hydrofluoric acid solution (HF, 40%) was added. The time of contact was 24 h in an oven at 50 °C.

20 mL of toluene was then added, and the suspension was stirred for 1 h at room temperature. Finally, 50 mL of boric acid (H_3BO_3, 4%) was added to neutralize the remaining HF [25]. The polymer was recovered by precipitation in methanol, analyzed by FTIR and compared to the FTIR spectra of Hyb.Mat.

Characterizations

X-ray fluorescence; The chemical compositions are determined by X-ray fluorescence (XRF) spectrometry Philips PW 2400 XRF. The samples were prepared by the method of fusion with LiB_4O_7.

CHN; elements C and N were determined by thermal conductivity through combustion in oxygen at 1050 °C under a stream of helium with the formation of CO_2 and NO_2. The separation of the two species is done on a chromatographic column.

The XRD measurements were carried out using a diffractometer (Philips diffractometer X'Pert Software) using Cu-K$_\alpha$ radiation ($\lambda = 0.1540$ nm) which includes an X tube with Cu anode powered by high frequency. A goniometer is equipped with a detector. A monochromator located on the diffracted beam is used to select the average wavelength of Cu. A computer is equipped with software for piloting the goniometer and counting and recording the results. We used a step of 0.02° and a counting time of 1.05 s/step, for a 2 θ

interval between 3 and 80°. The corresponding basal space was calculated by application of Bragg's law.

TGA; The analyses were carried out under a nitrogen flow at 10 mL min^{-1}, for a heating rate of 10 °C min^{-1} and a temperature interval of 30 to 800 °C, using a thermogravimetric analyzer of the SHIMADZU TGA brand − 51.

FTIR; The Fourier transform infrared FTIR spectra are recorded on a branded device (Shimadzu FTIR 830 spectrophotometer) with a spectral range of 4000 and 400 cm^{-1}. 297 mg of pure and dry KBr is mixed with 3 mg of solid product. The pellet is obtained by compression of the mixture under vacuum (8 tonnes cm^{-2}).

Results and discussion

Analysis of elements by XRF

The results of elements analysis by XRF are grouped in Table. 1

In order to better evaluate the cations exchanged with sodium cations in Mt-Na and nitrogen in Mt-DDA, to know the nature of the cations replaced during the exchanges, the ratios [Cation/Si] were calculated before and after both exchanges. The obtained results are mentioned in Table 2.

The compositions of raw Mt, Mt-Na and Mt-DDA were determined by XRF technique. The comparison between raw clay and sodic montmorillonite showed a decrease in Ca, K and Mg ratios after sodification of clay. But an increase in Na ratio was observed. The sum of decreasing ratios of Ca (50%), K (30%) and Mg (35%) was approximately equal to value of increasing ratio of Na (̃ 100%). This results showed a successful sodification of clay by exchange process and that the montmorillonite is the predominant phase in this clay.

The composition of the Mt-DDA showed clearly that the Na$^+$ cations were replaced by the –NH$_3^+$ cations of DDA salt during the modification (nitrogen ratio = 1.74%).

Table 1 XRF results of raw Mt, Mt-Na and Mt-DDA samples

Percentage of elements/%	Si	Al	Fe	Ca	Mg	S	K	Na
Raw Mt	25.26	9.39	2.45	0.88	3.03	0.16	0.97	1.45
Mt-Na	25.79	9.63	2.20	0.42	1.86	0.15	0.64	2.78
Mt-DDA	25.76	9.53	1.50	0.05	1.40	0.15	0.63	0.31

Table 2 Atomics reports [Cation/Si], before and after exchange by DDA salt

[Cation/Si]/%	Al/Si	Fe/Si	Ca/Si	Mg/Si	S/Si	K/Si	Na/Si
Mt-Na	37.34	8.53	1.62	7.25	0.58	2.48	10.77
Mt-DDA	36.99	5.82	0.19	5.43	0.58	1.40	1.20

These results were confirmed by the calculation of the [Cation/Si] ratios where a clear decrease in the [Na /Si] ratio from 10.77 to 1.20% is obtained after modification.

The other [Cation/Si] ratios have kept approximately constant values, so; these cations did not represent exchange sites.

Elements analysis by CHN method

The results obtained by this technique were for Mt-DDA, Mt-TMSPM and HO-M M and are grouped in Table 3 which showed a logical evolution of the carbon ratio during modification and grafting reactions.

XRD results

The XRD spectra of the five samples are represented in Fig. 1. It clearly showed the disappearance of some peaks presented in raw Mt related to impurities after the first modification process.

This is due to a successful washing, and purification process of the raw clay was achieved.

Despite the various treatments of raw Mt (purification, exchange with Na$^+$, modification by DDA, grafting and copolymerization), the main pics were not modified. Therefore, these treatment cannot lead to a significant change in the structure of clay.

These various treatments have changed only the interlayer spacing d_{001} of clay platelets (Table 4 and Fig. 1).

The raw clay showed several reflections in the angular range 2θ (2–10°) indicating the presence of various mono- and bihydrated cations and a predominance of montmorillonite with small amounts of impurities such as quartz, feldspat and traces of cristobalites [26].

The characteristic peak of montmorillonite displays a diffraction at $2\theta = 6.35°$, corresponding to a basal spacing $d_{001} = 13.90$ Å. This spacing represented the sum of the thickness of the TOT layer of montmorillonite (9.50 Å) [27] and the interlayer spacing which depends on the size of the cations and the interlayer water whose mass content was determined by TGA.

The Mt-Na showed a pic located at $2\theta = 6.96°$ ($d_{001} = 12.69$ Å), this decreasing in spacing value is mainly due to the substitution of the exchangeable cations K$^+$, Ca^{2+} and Mg^{2+} which were exchanged by the monovalent cations Na$^+$.

The increase in spacing d_{001} to 15.33 Å ($2\theta = 5.76°$) displayed by Mt-DDA confirms the

Fig. 1 XRD patterns of raw Mt (**a**), Mt-Na (**b**), Mt-DDA (**c**), Mt-TMSPM (**d**) and Hyb.Mat (**e**)

intercalation of alkylammonium cations between sheets of the montmorillonite.

It should be remembered that the possible arrangements of the alkylammonium ions intercalated in the interlayer spaces of the smectites can be in monolayer, in bilayer, in pseudo-trilayer and in paraffin structure arrangements [28] Scheme 2.

The length of DDA molecule was approximately 16.73 Å and the thickness was about 2.809 Å (values determined by the Chemsketch software, Scheme 3).

The interlayer space available is 5.83 Å, (15.33 Å– 9.50 Å). The cations adsorbed could therefore be intercaled in the galleries of montmorillonite in two layers horizontally superimposed ($2 \times 2.809 \cong 5.83$ Å).

The functionalization of Mt-DDA was carried out by grafting of TMSPM molecules carrying methoxy –OCH$_3$ groups as a hydrolyzable alkoxy group and the methacrylic function as an organo-functional group.

If the TMSPM silane was interacted with the clay mineral surface, forming chemical bonds at the interface, it must be first converted to reactive silanol by hydrolysis. This hydrolysis can occur directly on the surface of the substrate by reaction with the surface water (direct hydrolysis) or during a previous step of preparation of the aqueous silane solution (prehydrolysis).

Table 3 CHN results of Mt-DDA, Mt-TMSPM and Hyb.Mat samples

Sample	Mt-DDA	Mt-TMSPM	HO-MM
%C	5.30	7.80	19.30
%N	1.74	–	–

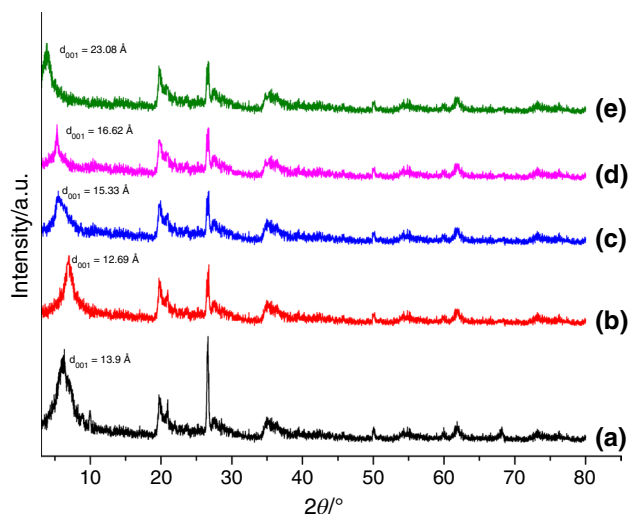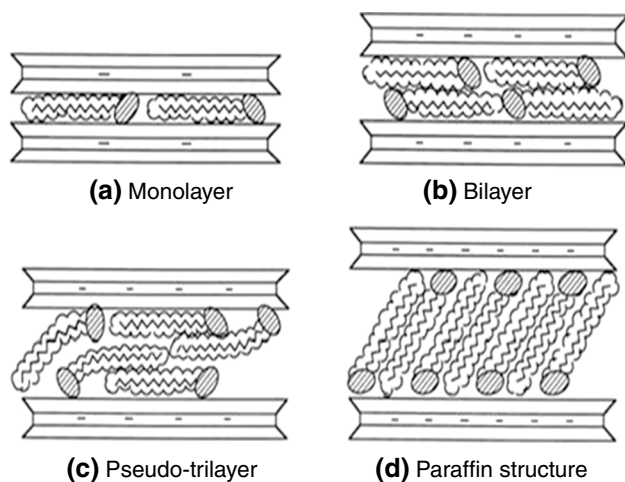**Table 4** Values of 2θ (001 reflexion) and d_{001} of five samples

Samples	Raw Mt	Mt-Na	Mt-DDA	Mt-TMSPM	HO-M M
2θ	6.35	6.96	5.76	5.31	3.82
d_{001} (Å)	13.90	12.69	15.33	16.62	23.08
Spectra	(a)	(b)	(c)	(d)	(e)

(a) Monolayer

(b) Bilayer

(c) Pseudo-trilayer

(d) Paraffin structure

Scheme 2 Representation of different conformations of alkylammonium cations onto clay galleries: Monolayer (**a**), Bilayer (**b**), Arrangement pseudotrimoleculaire (**c**) and paraffined structure (**d**)

The silanol form of the silane can be grafted onto clay mineral by reaction of condensation with the hydroxyl groups on the montmorillonite surface, in this case, the methacrylic functions will be found between sheets of the clay. This would increase the hydrophobicity of the montmorillonite.

The XRD spectra of Mt-TMSPM revealed a basal spacing $d_{001} = 16.62$ Å greater than 15.33 Å displayed by the Mt-DDA. In addition to grafting reaction of silane molecules on silanol Si–OH of the sheets edges of montmorillonite, this increase in d_{001} is an advance of another hypothesis for reaction type, that is the condensation of the hydroxyl groups of surface with silane molecules whose alkoxy groups are hydrolyzed by interlamellar hydration water. This deduction is in perfect agreement with the results of the study realized by [23] which concluded

that the grafting reactions of silanes on montmorillonites strongly depend on its concentration.

This study showed that grafting can occur on the silanols of sheets edges and those on the hydroxylated surfaces, for silanes concentration of 3 mmol/g of montmorillonite.

This exactly coincides with an amount 8 mL ($\approx$ 8 g) of TMSPM ($M = 248.08$ g mol^{-1} and a density $= 1.045$ g mL^{-1}) added to 10 g of clay.

On the XRD spectra of hybrid material Hyb.Mat, a first pic located at $2\theta = 3.82°$ ($d_{001} = 23.08$ Å) was observed. An increase of 6.46 Å compared to d_{001} of the Mt-TMSPM was observed, which can only be explained by the presence of macromolecular chains of the copolymer (the copolymerized monomer of styrene with the methacrylic double bond carried by the TMSPM) onto clay galleries. In addition, the pic intensity related to 001 reflexion is unchanged, this indicated the presence of a quantity of PS in the interlayer space (existence of intercalated structure).

TG results

The both thermogravimetric (TG) and its derivative (DTG) curves, in inert atmosphere, of five samples are represented in Fig. 2.

The (TGA and DTG) curves of raw Mt sample (Fig. 2a) revealed two degradations steps. The first mass loss is located at the temperature range (30–250 °C) with a maxima at 133 °C evaluated at 09.54% attributed to the desorption of physically adsorbed water and to dehydration of interlayer hydrated cations. The second range (600–750 °C) with a maxima at 700 °C displayed the mass loss of 03.29%, attributed to dehydroxylation of the aluminosilicate sheets [29].

The (TGA and DTG) curves of Mt-Na sample (Fig. 2b) also revealed two degradations steps. The first mass loss is located at the same temperature range (30–250 °C) with a maxima at 128 °C evaluated at 11.46% attributed to the

Scheme 3 Representation of DDA molecule size determined by the Chemsketch software
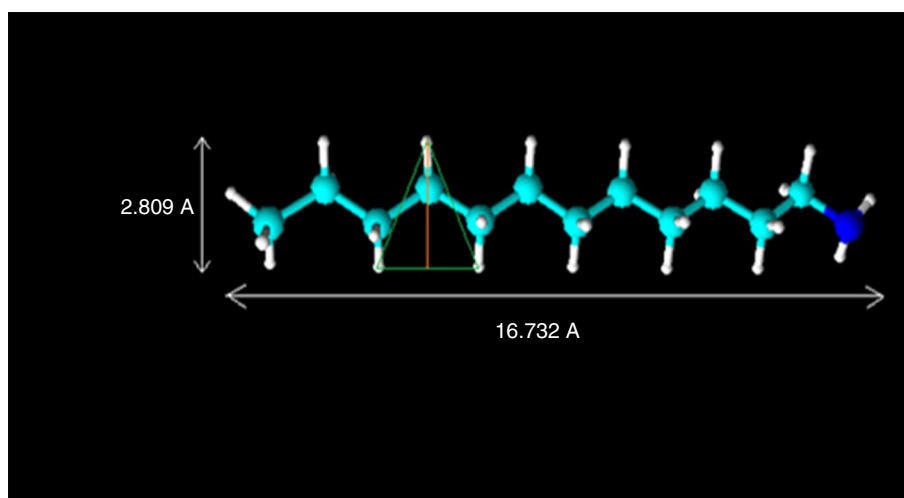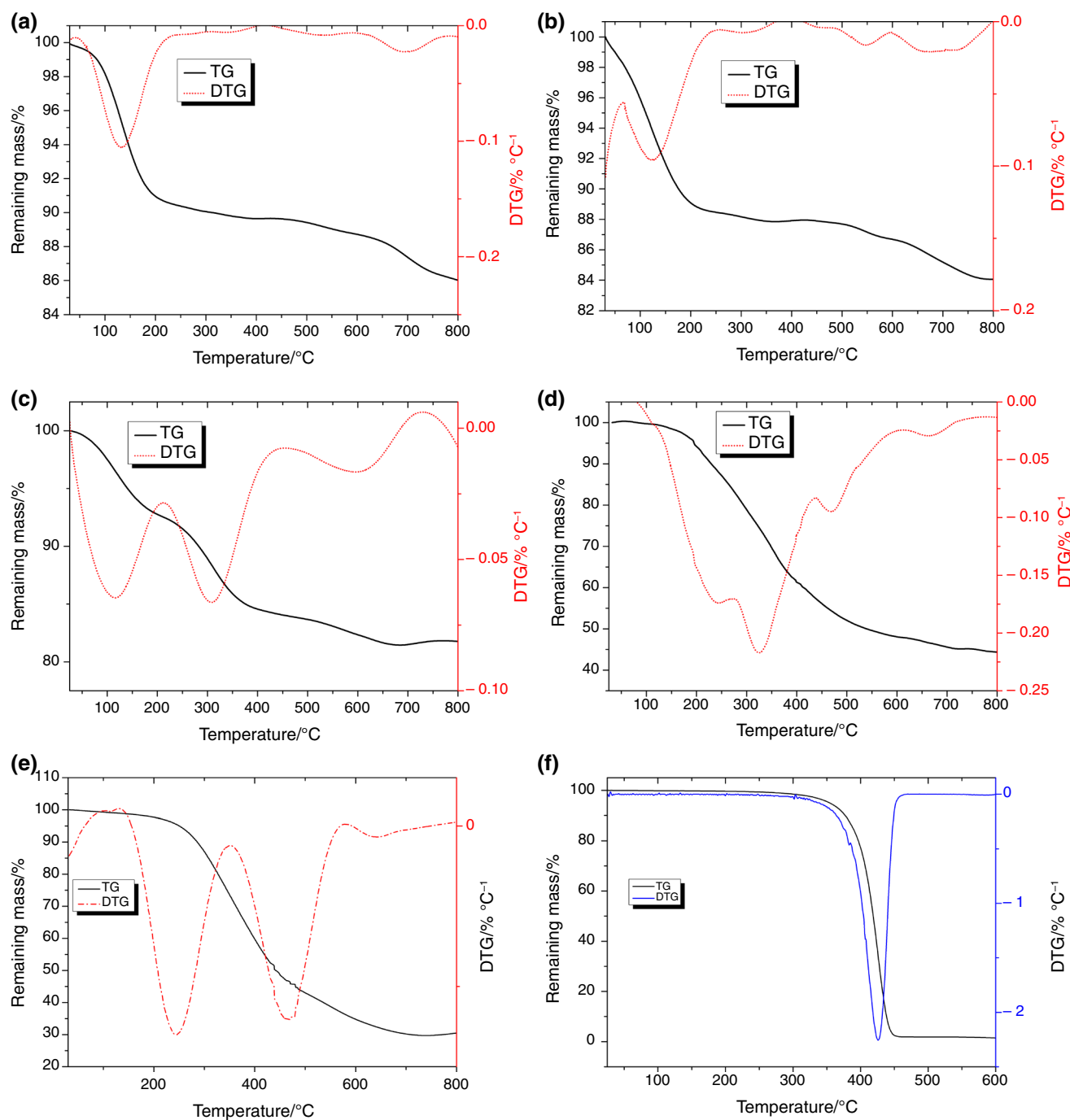
Fig. 2 TG, DTG curves of raw Mt (**a**), Mt-Na (**b**), (MMT-DDA) organomontmorillonite (**c**), (MMT-TMSPM) double organomontmorillonite (**d**), (Hyb.Mat) (**e**) and hybrid material (**f**)

desorption of physically adsorbed water and to dehydration of interlayer hydrated cations. The second range (600–750 °C) with a maxima at 675 °C displayed the same mass loss of 03.84%, attributed to dehydroxylation of the aluminosilicate sheets. These results correspond to those found by the elements analysis (losses on fire).

The mass loss displayed by Mt-Na in the range (30–250 °C) was higher than raw Mt, this can be explained by the high number of water molecules entered the Na$^+$ ions compared to other cations (Ca^{2+}, Mg^{2+} and K$^+$) because Na$^+$ is more hydrated.

The (TG and DTG) curves of the Mt-DDA (Fig. 2c) presented three degradations steps. The first mass loss in the ranges (30–210 °C) with a maxima at 113 °C, the second (210–450 °C) with a maxima at 290 °C and the last (500–700 °C) with a maxima at 600 °C is evaluated at 07.14%, 09.15% and 02.29%, respectively, which correspond to release of physisorbed water, to decomposition of DDA and to dehydroxylation phenomenon, respectively.

The mass loss 07.14% is lower than the values displayed by the first two samples in the same temperature range, this is an indication of a decrease in the water molecules adsorbed in the interlayer of montmorillonite and confirms the exchange of hydrated cations Na^+ by DDA cations. [30, 31].

In previous study, a pur HDTMA is having more number of carbon than DDA, the decomposition of this surfactant occurred in the range of temperature (200–350 °C) with a maxima at 269 °C [14], whereas the decomposition of DDA intercaled clay over on large temperature range (210–450 °C), with a maxima at 290 °C, passed 30 min, taking into account the heating rate of 10 °C/min (TGA operating conditions), this slow decomposition proves that the intercalation of alkylammonium molecules in gallery of clay retards their decompositions, this is indirectly a favor of intercalation efficiency process. The last degradation step located in the range (500–700 °C) with a maxima at 600 °C displayed the mass loss of 2.29%, attributed to dehydroxylation of the aluminosilicate sheets.

The (TG and DTG) curves of Mt-TMSPM sample (Fig. 2d) also showed three degradations steps; the first (30–190 °C) with a maxima at 113 °C, the second (190–600 °C) with three maxima and the last (600–750 °C) with a maxima at 670 °C estimated at (05.92%), (48.95%), (06.12%), respectively. In the first temperature range, the water content was more decreased from 07.14% for the Mt-DDA to 05.92% for the Mt-TMSPM. This decreasing is the result of pronounced hydrophobicity of Mt-TMSPM sample, caused by the presence of grafted organic chains of TMSPM at the layers of montmorillonite. Another detail is worth noting for the mass loss 05.92% of the Mt-TMSPM, which confirms the presence of TMSPM between the sheets, following the hydrolysis reaction of its hydrophilic end groups.

The second degradation step showed three mass loss, the first is in the range (190–275 °C) with a maxima at 245°C evaluated at 13% which corresponds to the onset decomposition temperature of silane grafted on the layered silicate [13]. The second mass loss is in the range (275–435 °C) with a maxima at 327 °C evaluated at 25% is attributed to the decomposition of DDA and second decomposition step of TMSPM. The third mass loss is in the range (435–600 °C) with a maxima at 470 °C evaluated at 10% which corresponds to last decomposition step of TMSPM. The last degradation step located in the range (600–750 °C) with a

maxima at 670 °C displayed the mass loss of 6.12%, attributed to dehydroxylation of the aluminosilicate sheets.

Furthermore, the decomposition process of the Mt-TMSPM was slower than that of the Mt-DDA (more large temperature range than Mt-DDA), and a higher mass loss, which can be attributed to the grafting of silane molecules, with higher thermal stability based on the Mt-DDA. Results on the thermal stability of materials provided additional evidence that the grafting of TMSPM at montmorillonite layers was successful.

The (TG and DTG) curves of Hyb.Mat sample (Fig. 2e) also showed three degradations steps; the first (30–135 °C), the second (135–580 °C) with two maxima and the last (580–750 °C) with a maxima at 645°C estimated at 1.5%, 62.8% and 5.5%, respectively. In the first temperature range, the water content was more decreased from 05.92% for Mt-TMSPM to 1.5% for the Hyb.Mat. This decreasing is the result of pronounced hydrophobicity of hybrid material, caused by the presence of organic chains of polymer in the surface of montmorillonite.

The second one (135–580 °C) revealed two mass loss, the first in the range (135–350 °C) with a maxima at 245 °C estimated at 25.30% attributed to the onset decomposition of TMSPM and decomposition od DDA. The second in the range (350–580 °C) with a maxima at 470 °C estimated at 37.5% is mainly attributed to degradation of polystyrene polymer and the two last decomposition steps of TMSPM. The last degradation step located in the range (580–750 °C) with a maxima at 645 °C displayed the mass loss of 5.5%, attributed to dehydroxylation of the aluminosilicate sheets.

The (TG and DTG) curves of pure Ps sample (Fig. 2f) showed only one degradation step which occurred in the first (330–455 °C) with a maxima at 424°C and total degradation in this range of temperature.

The (TG/DTG) results are summarized in Table 5.

Thermal stability of hybrid material

The thermal stability of the Hyb.Mat hybrid material and the prepared pure Polystyrene polymer was studied.

The onset decomposition temperatures ($T_{5\%}$) (5% mass loss temperature), the mid-point decomposition temperatures ($T_{50}\%$) (50% mass loss temperature), the maximum and finally mass loss temperatures (T_{max} and T_f obtained from DTG) of two materials are listed in Table 6.

At ($T_{5\%:}$), a decrease of 82 °C was noticed in Hyb.Mat compared to pure Ps, which can be explained by the higher content of organic modifiers (both DDA and TPMS) that can be decomposed easily in the early stage of thermal degradation, resulting in the lower onset decomposition temperature;

At $T_{50\%}$ (°C); the $T_{50\%}$ was 29 °C higher for the Hyb.Mat than that observed for the pure Ps.

Table 5 TG/DTG results

	Raw Mt	Mt-Na	Mt-DDA	Mt-TMSPM	Hyb.Mat	PS$_{pure}$
1st Variation	30–250 °C	30–250 °C	30–210 °C	30–190 °C	30–135 °C	–
Maxima	133 °C	128 °C	113 °C	113 °C	118 °C	
Loss of mass	9.54%	11.46%	7.14%	5.92%	1.50%	
2nd Variation	–	–	210–450 °C	190–275 °C	135–350 °C	330–455 °C
Maxima	–	–	290 °C	245 °C	245 °C	424 °C
Loss of mass	–	–	9.15%	13%	25.30%	98%
				275–435 °C	350–580 °C	–
Maxima				327 °C	470 °C	
Loss of mass				25%	37.50%	–
				435–600 °C		
Maxima				470 °C	–	
Loss of mass				10%		
3rd Variation	600–750 °C	600–750 °C	500–700 °C	600–750 °C	580–745 °C	–
Maxima	700 °C	675 °C	600 °C	670 °C	645 °C	
Loss of mass	3.29%	3.84%	2.29%	6.12%	5.50%	

Table 6 TGA data of pure PS polymer and Hyb.Mat at different decomposition temperatures ($T_{5\%}$, $T_{5\%}$, T_{max} and T_f)
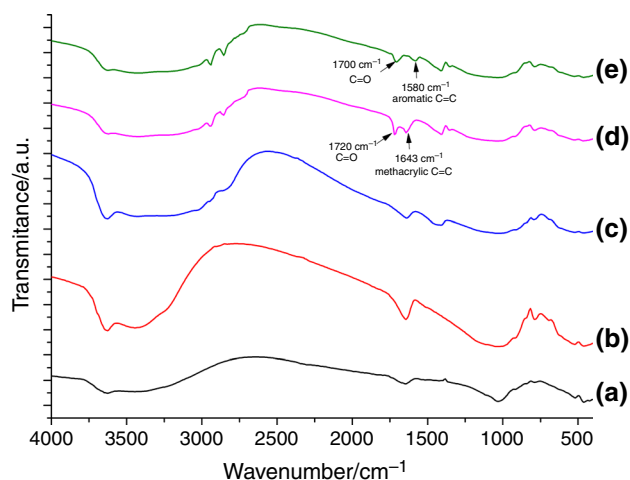
Sample	$T_{5\%}$/°C	$T_{50\%}$/°C	T_{max}/°C	T_f/°C
Pure Ps	352	416	425	445
Hyb.Mat	270	445	470	580

Fig. 3 FTIR spectra of raw Mt (**a**), Mt-Na (**b**), Mt-DDA (**c**), Mt-TMSPM (**d**) and Hyb.Mat (**e**)

Also, in the DTG curves, the T_{max} of the Hyb.Mat was greatly higher than Ps (45 °C higher).

At the end of decomposition process, the T_f of Hyb. Mat was 135 °C higher than pure Ps.

These indicated that the organoclay exhibited a beneficial effect on the enhancement of thermal stability of Ps. This great enhancement of thermal stability may be that the amount of intercalated Ps is high enough to promote high thermal stability of polymer, which acts as a physical barrier preventing the heat to propagate quickly and delaying its decomposition. The TG analysis confirms the result obtained by XRD that showed the majority intercalated polymer in the clay galleries. Samakande et al. [32] observed similar results with Ps/clay nanocomposites prepared by free-radical polymerization in bulk. In their work, it is clear that a higher degree of intercalation of polystyrene polymer in clay galleries led to the improvement of the Ps/clay nanocomposite's thermal stability.

Greesh et al. [33] compared thermal stabilities of intercaled and exfoliated Ps/ MPTMS grafted Na-MMT nanocomposites who found higher thermal stabilities for intercalated structures relative to the exfoliated morphologies.

FTIR results

The FTIR spectra of five samples (raw Mt, Mt-Na, Mt-DDA, Mt-MPTMS and Hyb.Mat) are regrouped in Fig. 3. The characteristic bands of raw Mt (Fig. 3a) with their respective attributions are grouped in Table 7.

For Mt-Na spectra (Fig. 3b), the intensity of OH bands (OH of water) was increased to a large extent due to the intercalation of Na$^+$ cations, leading to the formation of more hydrophile surface.

In the Mt-DDA spectra (Fig. 3c), the majority of the raw Mt bands were preserved, but new bands located at 2954.7 cm^{-1} and 2854.4 cm^{-1} appeared attributed to stretching vibrations of CH and CH$_2$ from the alkyl chain, respectively [34]. The bands located at 3201 cm^{-1} and 1420 cm^{-1}

Table 7 Main bands appeared in raw Mt FTIR spectra with their attributions

| Raw Mt sample ν/cm^{-1}	Attributions
3625.90	Stretching vibrations of O–H layers
3440.70	H–O–H stretching vibrations of physorbed water
1650.90	H–O–H binding of physorbed water
1033.70	Si–O binding
925.76	Al–Al–OH vibrations
840.90	Mg–Al–OH vibrations
786.90	Mg–Fe–OH vibrations
617.17	Al–O–H vibrations
524.60	Si–O–Al vibrations
462.88	Si–O vibrations
424.31	Si–O–Si Vibrations

Fig. 4 FTIR spectra of recovered copolymer by HF attack (**a**), and hybrid material (Hyb.Mat) (**a′**)

can be assigned, respectively, to the N–H stretching and binding of ammonium [35].

In comparison with the Mt-Na spectra (Fig. 3b), the decrease in intensities of the bands at 3440 cm^{-1} and 1635.5 cm^{-1} related to OH hydration water was noticed, because the hydrated cations initially present in the interlayer space (Na^{+}) were substituted by DDA cations during the cation exchange process, which transform the surface of clay from hydrophile to hydrophobe state, this means that the intercalation of montmorillonite by the alkyammonium produces less space available for adsorption of water molecules, so the intercalation by DDA has taken place.

The spectra of Mt-TMSPM sample are represented in Fig. 3d. In addition to the characteristic bands of the mentioned samples (raw Mt, Mt-Na and Mt-DDA), the spectra of grafted clay showed other bands located at 1643 cm^{-1} and 1720 cm^{-1} assigned, respectively, to: C=C and C=O of the TMSPM molecules.

The higher intensities of the absorption bands at 2939.3 and 2854.4 cm^{-1} compared to Mt-DDA sample were also observed, which confirmed that the TMSPM was successfully grafted onto the silanol of montmorillonite sheets [36].

The significant decrease in band intensity located at 3625.9 cm^{-1}, which attributed to OH of the silanols Si–OH and the aluminols Al–OH located at the edges of the tetrahedrons and octahedra of montmorillonite sheets in the Mt-TMSPM sample compared to that in the Mt-DDA, can be explained by the conversion of the silanol Si–OH to Si–O–Si during grafting process with the silane(Scheme 1a), this observation is another confirmation of grafting that is not noticed by the previous studies. It is an important remark for confirmation of grafting reaction. The almost total disappearance of the band located at 1635.5 cm^{-1} was also observed, which implies a decrease in the water content
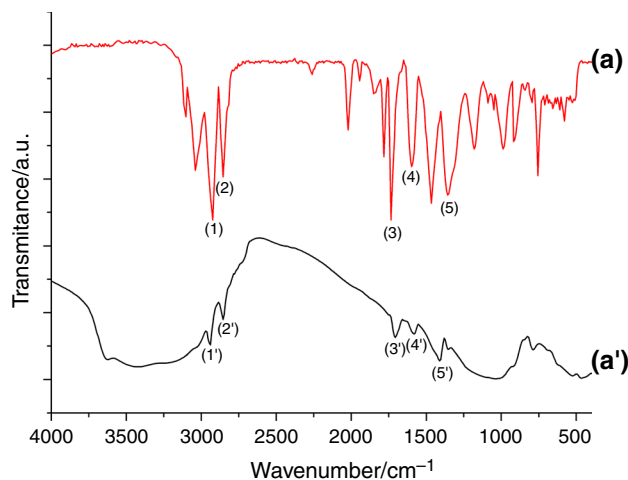
and a more change of the montmorillonite surface from its hydrophilic state to a hydrophobic one.

In the Hyb.Mat spectra (Fig. 3e), a band at 1580 cm^{-1} attributed to aromatic C=C of styrene was appeared.

The bands related to C=O and C=C groups of silane before polymerization were located at 1720 cm^{-1} and 1643 cm^{-1}, respectively. After polymerization, an important remark was noticed that the absence of band related to C=C methacrylic double bond is copolymerized with styrene monomer (Scheme 1b). This is another important confirmation of copolymerization reaction that was also not noticed by the previous studies. The C=O group of the ester, lose its conjugation with the double bond, absorbs at 1700 cm^{-1}, frequency may be high for an unconjugated aliphatic ester, this lowering of the wave number is due to the donor character of the aromatic cycle favoring a certain electronic density around the group C=O.

Dissolution of hybrid material by HF attack

The attack of Hyb.Mat by hydrofluoric acid leads to recover the copolymer (methacrylate–styrene) initially grafted and to highlight in the FTIR spectra in Fig. 4.

The superposition of the two spectra clearly showed common analogous bands designated by (1.1′ at 2954.7 cm^{-1}), (2.2′ at 2854 cm^{-1}), (3.3′ at 1700 cm^{-1}), (4.4′ at 1580 cm^{-1}) and (5.5′ at 1356 cm^{-1}) attributed, respectively, to the vibrations of the C–H (alkyl chain), CH$_2$(alkyl chain), C=O (silane), (aromatic C=C of styrene) and methacrylate C–O–C groups. it is important to notice the appearance; on the spectrum (a) of a series of bands in the interval 1200–400 cm^{-1} which were masked by the silicic framework in the Hyb.Mat before the HF attack.

Conclusions

To prepare an organoclay hybrid material, the grafting of monomer (styrene type) by radical copolymerization onto Algerian montmorillonite exchanged by an alkylammonium (DDA salts) and functionalized beforehand by a silane (TMSPM) carrying an adequate chemical function allowing the copolymerization of the monomer at the surface of clay was realized. Various physicochemical characterizations using XRF, CHN, XRD, TGA and FTIR have demonstrated; the intercalation of DDA salts by enhancement of interlayer space of clay; the grafting of TMSPM by creation of the new covalent bond Si–O–Si between the clay surface and the silane and the grafting of macromolecule polymer with the functionalized silane. These results of characterization revealed also the higher thermal stability of prepared organoclay hybrid material compared to pristine polystyrene polymer and the strong hydrophobicity of its area.

We have just exposed a series of original results characterizing the behavior of organoclay hybrid material manifesting an intercaled structure, very pronounced thermal stability and hydrophobic character.

References

1. Zhao Q, Choo H, Bhatt A, Burns SE, Bate B. Review of the fundamental geochemical and physical behaviors of organoclays in barrier applications. Appl Clay Sci. 2017;142:2–20.
2. Arellano-Cardenas S, Lopez-Cortez S, Cornejo-Mazon M, Carlos M-G. Study of malachite green adsorption by organically modified clay using a batch method. Appl Surf Sc. 2013;280:74–8.
3. Emerson PB, Mariana SL, Isabelle BA, Pedro MB, Jo D. Partially exchanged organophilic bentonites Part II. Phenol adsorption. J Therm Anal Calorim. 2011;105:915–20.
4. Sousna S, Mokhtar B, Chafia T, Abdelkrim K. Adsorption of tartrazine from an aqueous solution by octadecyltrimethylammonium bromide-modified bentonite: kinetics and isotherm modeling. C R Chim. 2018;21:391–8.
5. Lei L, Xiaoxuan X. Polystyrene nanocomposites with improved combustion properties by using TMA-POSS and organic clay. J Therm Anal Calorim. 2016;124:743–9.
6. Xiang W, Qiang S, Yumei H, Chuanzeng W, Junping Z. Structure and thermal stability of PMMA/MMT nanocomposites as denture base material. J Therm Anal Calorim. 2014;115:1143–51.
7. Wang P, Yang F, Cai Z. Synergistic effect of organo-montmorillonite and DOPO-based oligomer on improving the flame retardancy of epoxy thermoset. J Therm Anal Calorim. 2017;128:1429–41.
8. Long Y, Zhisheng X, Jun Z. Influence of nanoparticle geometry on the thermal stability and flame retardancy of high-impact polystyrene nanocomposites. J Therm Anal Calorim. 2017;130:1987–96.
9. Li ZH, Bowman RS. Sorption of chromate and PCE by surfactant-modified clay minerals. Environ Eng Sci. 1998;15:237–45.
10. Zhang YX, Zhao Y, Zhu Y, Wu HY, Wang HT, Lu WJ. Adsorption of mixed cationic-nonionic surfactant and its effect on bentonite structure. J Environ Sci. 2012;24:1525–32.
11. Tuchowska M, Muir B, Kowalik M, Socha RP, Bajda T. Sorption of molybdates and tungstates on functionalized montmorillonites: Structural and textural features. Materials. 2019;12:21.
12. Bergaya F, Lagaly G, Vayer M. Cation and anion exchange. In: Bergaya F,Theng BKG, Lagaly G (eds) Handbook of clay science, 1st edn. Elsevier, Amsterdam; Vol 1.2006;979–1001
13. Herrera NN, Letoffe JM, Putaux JL, David L, Bourgeat-Lami E. Aqueous dispersions of silane-functionalized laponite clay platelets. A first step toward the elaboration of water-based polymer/clay nanocomposites. Langmuir. 2004;20:1564–71.
14. Zorica P, Tomic Lazar K, Natasa N, Smilja M, Petre M. Thermal investigation of acetochlor adsorption on inorganic- and organic-modified montmorillonite. J Thermal Anal Calorim. 2016;123:2313–9.
15. Zhang ZH, Li TS, Yang F, Fu CG. Montmorillonite clay catalysis XI: protection and deprotection of hydroxyl group by formation and cleavage of trimethylsilyl ethers catalysed by montmorillonite K-10. Synth Commun. 1998;28:3105–14.
16. Ogawa M, Okutomo S, Kuroda K. Control of interlayer microstructures of a layered silicate by surface modified cation with organochlorosilanes. J Am Chem Soc. 1998;120:7361–2.
17. Asgari M, Sundararaj U. Silane functionalization of sodium montmorillonite nanoclay: the effect of dispersing media on intercalation and chemical grafting. Appl Clay Sci. 2018;153:228–38.
18. Bertuoli PT, Piazza D, Scienza LC, Zattera AJ. Preparation and characterization of montmorillonite modified with 3-aminopropyltriethoxysilane. Appl Clay Sci. 2014;87:46–51.
19. Park M, Shim IK, Jung EY, Choy JH. Modification of external surface of laponite by silane grafting. J Phys Chem Solids. 2004;65:499–501.
20. Wei S, HongPing H, JianXi Z, Peng Y, YueHong M, XiaoLiang L. Preparation and characterization of 3-aminopropyltriethoxysilane grafted montmorillonite and acid-activated montmorillonite. Chin Sci Bull. 2009;54:265–71.
21. Romanzini D, Piroli V, Frache A, Zattera AJ, Amico SC. Sodium montmorillonite modified with methacryloxy and vinylsilanes: Influence of silylation on the morphology of clay/unsaturated polyester nanocomposites. Appl Clay Sci. 2015;114:550–7.
22. Su L, Tao Q, He H, Zhu J, Yuan P, Zhu R. Silylation of montmorillonite surfaces: dependence on solvent nature. J Colloid Interf Sc. 2013;391:16–20.
23. Wentao H, Yong Y, Min H, Zhang K, Lijuan L, Minmin Z, Shuhao Q, Yu J. Influence of reaction conditions on the grafting pattern of 3-glycidoxypropyl trimethoxysilane on montmorillonite. Bull Korean Chem Soc. 2013;34:112.
24. Revillon A, Leroux D. Functional silica supported polymer V. 'Onto' versus 'from' grafting processes. React Funct Polym. 1995;26:105–18.
25. Chartier A, Gonnet C, Morel D, Rocca JL, Serpinet J. Mixed bonded phases for high-performance liquid chromatography: I. Synthesis and physico-chemical characterization. J Chromatogr A. 1988;438:263–71.
26. Jesús Fernández M, Dolores Fernández M, Aranburu I. Effect of clay surface modification and organoclay purity on microstructure and thermal properties of poly (L-lactic acid)/ vermiculite nanocomposites. Appl Clay Sci. 2013;80–81:372–81.
27. Gulten A, Kadir YM. Nonyl-and dodecylamines intercalated bentonite and illite from Turkey. Turk J Chem. 1999;23:105–13.
28. Lagaly G. Characterization of clays by organic compounds. Clay Miner. 1981;16:1–21.
29. Elkhalifah A, Maitra S, Bustam MA, Murugesan T. Thermogravimetric analysis of different molar mass ammonium cations

intercalated different cationic forms of montmorillonite. J Therm Anal Calorim. 2012;110:765–71.

30. He H, Ding Z, Zhu J, Yuan P, Xi Y, Yang D, Frost LR. Thermal characterization of surfactant-modified montmorillonites. Clays Clay Miner. 2005;53:287–93.

31. Zidelkheir B, Abdelgoad M. Effect of surfactant agent upon the structure of montmorillonite, X-ray diffraction and thermal analysis. J Therm Anal Cal. 2008;94:181–7.

32. Samakande A, Hartmann PC, Cloete V, Sanderson RD. Use of acrylic based surfmers for the preparation of exfoliated polystyrene-clay nanocomposite. Polymer. 2007;48:1490–9.

33. Nagi G, Hartmann PC, Sanderson RD. Preparation of polystyrene/clay nanocomposites by free-radical polymerization in dispersion. Macromol Mater Eng. 2009;294:787–94.

34. Ladjal N, Zidelkheir B, Terchi S. Influence of actadecylammonium, N, N-dimethylhexadecylammonium and 1-hexadecyltrimethylammonium chloride upon the fractionated montmorillonite. J Therm Anal Cal. 2018;134:881–8.

35. Aranda P, Ruiz-Hitzky E. Poly (éthylène oxide)/NH_4^+-smectite nanocomposite. Appl Clay Sci. 1999;15:119–35.

36. Park S, Kim B, Seo D, Rhee K, Lyu Y. Effects of a silane treatment on the mechanical interfacial properties of montmorillonite/epoxy nanocomposites. Mater Sci Eng A. 2009;526:74–8.